

Assignment 1

BEM Wind Turbine

Carlos Espinós Garcia
Niklas Perujo
Bernat Serra Zueras

Rotor and Wake Aerodynamics



Contents

1	Introduction	1
1.1	Assignment BEM BERNAT	1
1.2	Single polar innacuracies BERNAT	1
2	Blade Element Momentum theory	3
2.1	Main assumptions of the BEM theory NIKLAS	3
2.2	Code flow chart CARLOS	3
3	Results	5
3.1	BEM aligned rotor BERNAT	5
3.1.1	Main outputs BERNAT	5
3.2	BEM yawed rotor NIKLAS	5
3.2.1	Main outputs NIKLAS	5
3.3	Influence of the tip correction CARLOS	5
3.4	Influence of numerical discretization BERNAT	9
3.5	Evaluation of stagnation enthalpy CARLOS	9
3.6	System of circulation and vorticity CARLOS	13
3.7	Operational point NIKLAS	13
4	Optional	15
4.1	Explanation of the design approach used for maximizing the C_p or efficiency	15
4.2	Plots with explanation of the new designs.	15
5	Conclusions NIKLAS	17
	Bibliography	19

1

Introduction

1.1. Assignment BEM **BERNAT**

Blabla

1.2. Single polar innacuracies **BERNAT**

Chowchow

2

Blade Element Momentum theory

2.1. Main assumptions of the BEM theory **NIKLAS**

Perujo

2.2. Code flow chart **CARLOS**

CS7. Carlos Simao 7, ô magnifico

3

Results

Describe the initial conditions, table, cool

3.1. BEM aligned rotor **BERNAT**

3.1.1. Main outputs **BERNAT**

Angle of attack and inflow angle **BERNAT**

Axial and azimuthal inductions **BERNAT**

Thrust and azimuthal loading **BERNAT**

Total thrust and torque **BERNAT**

3.2. BEM yawed rotor **NIKLAS**

The results in this section were obtained for the rotor operating with tip speeds $\lambda = 6, 8, 10$ and yaw values of $\psi = 15, 30$ degrees.

3.2.1. Main outputs **NIKLAS**

Angle of attack and inflow angle **NIKLAS**

Axial and azimuthal inductions **NIKLAS**

Thrust and azimuthal loading **NIKLAS**

Total thrust and torque **NIKLAS**

3.3. Influence of the tip correction **CARLOS**

The results shown in this section were obtained for the rotor described in the assignment instructions, operating with a tip speed ratio $\lambda = 8$ and no yaw. It can be seen that the tip correction reduces the power and thrust, resulting in a worse performance. Indeed, the rotor without the tip correction has a higher C_P/C_T ratio.

Near the blade tip, the flow angle ϕ is reduced due to the tip vortex (Figure 3.7), because it induces a larger axial velocity (Figure 3.9). Having a lower flow angle ϕ results in a reduced power extraction, which is proportional to $c_l \sin \phi - c_d \cos \phi$ (Figure 3.10) [1]. However, reducing the flow angle ϕ contributes to an increase of the thrust, since it is proportional to $c_l \cos \phi + c_d \sin \phi$.

Note that c_l also decreases due to the reduction of ϕ , because it implies a decrease of the angle of attack α (Figure 3.8). Moreover, the relative velocity, which also affects the loads, will also be larger for the case without tip correction.

Table 3.1: CT and CP for yaw angle of 15 degrees.

	tsr 6	tsr 8	tsr 10
CT	0.4789	0.6359	0.7467
CP	0.3438	0.4234	0.4367

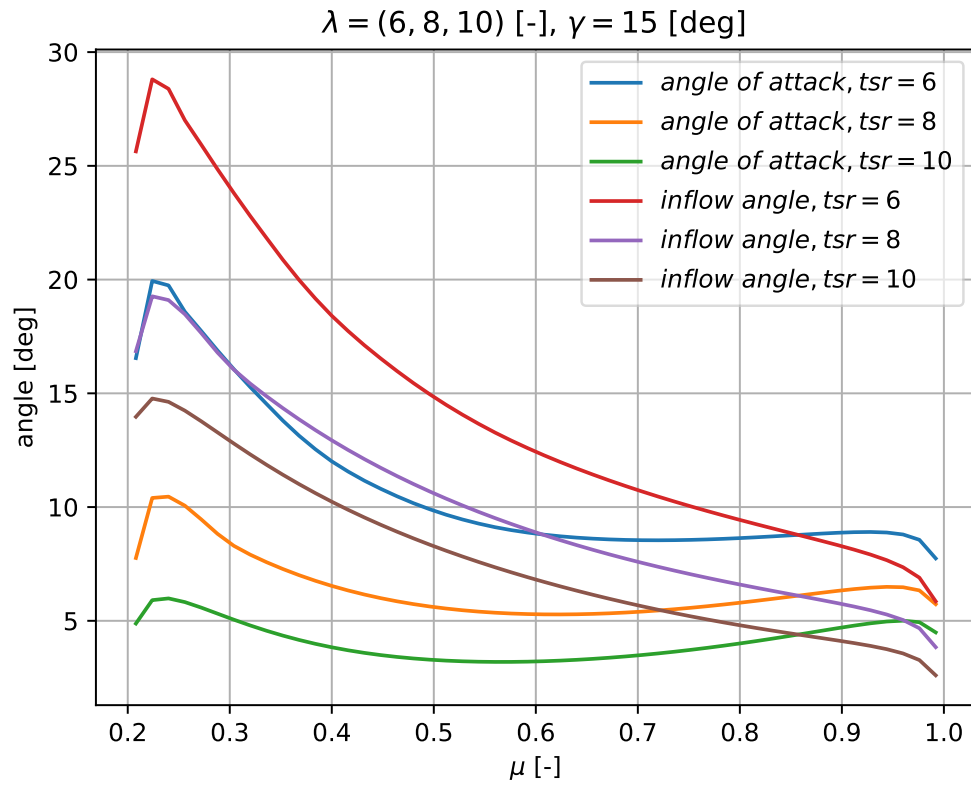


Figure 3.1: Angle of attack and inflow angle at a yaw of 15 degrees.

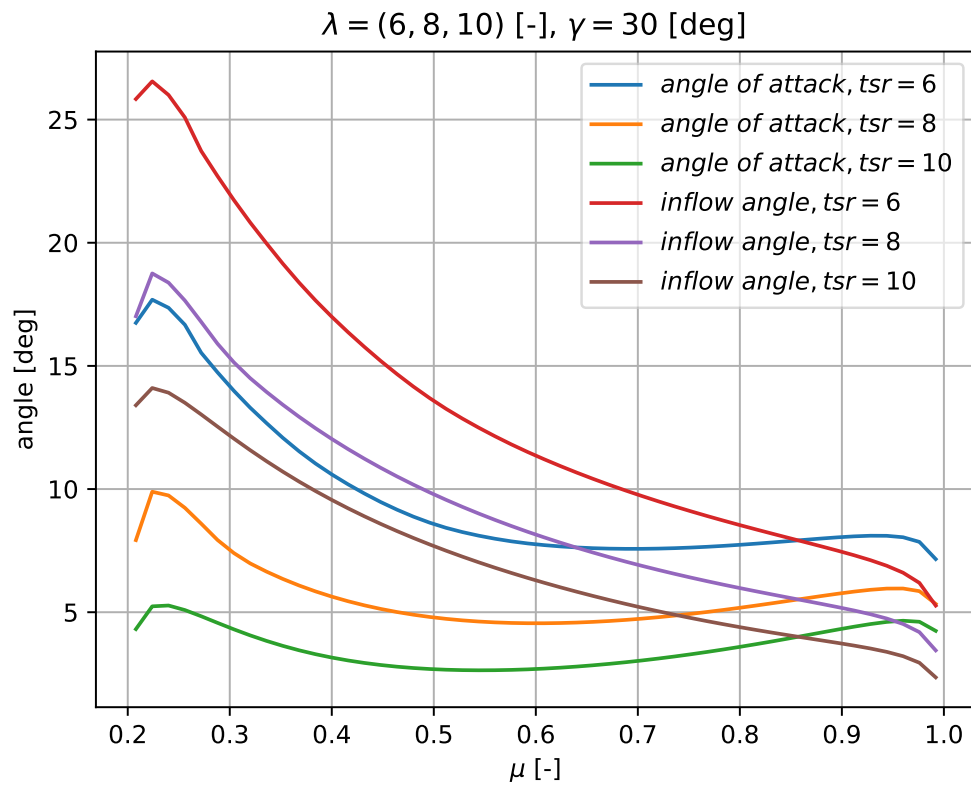


Figure 3.2: Angle of attack and inflow angle at a yaw of 30 degrees.

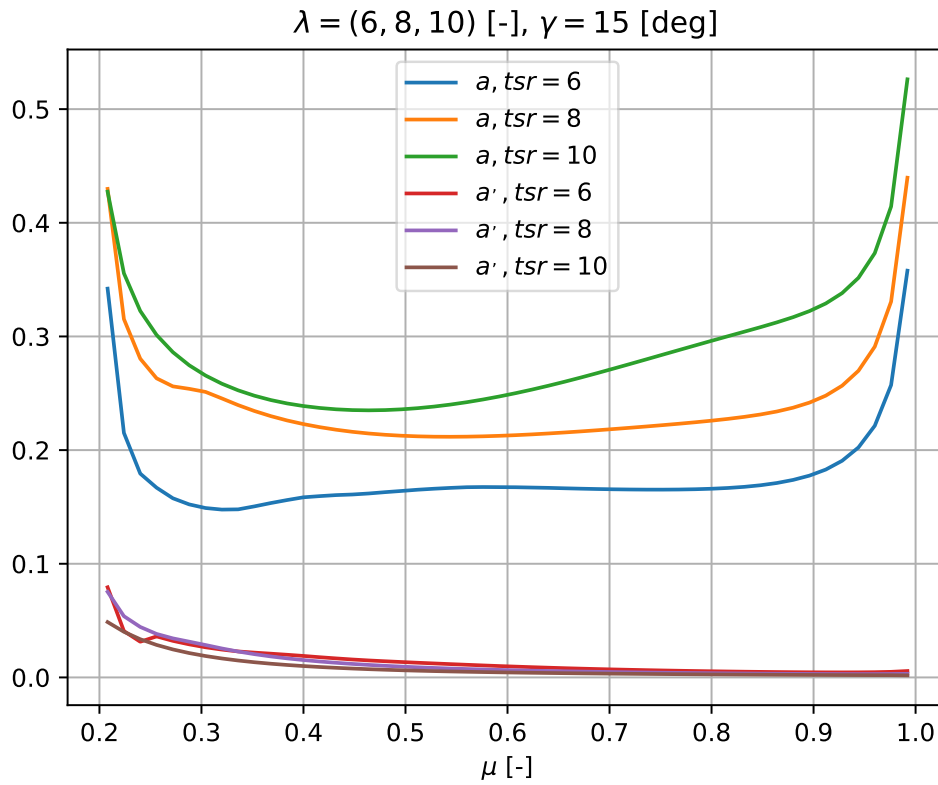


Figure 3.3: Axial and azimuthal inductions at yaw of 15 degrees.

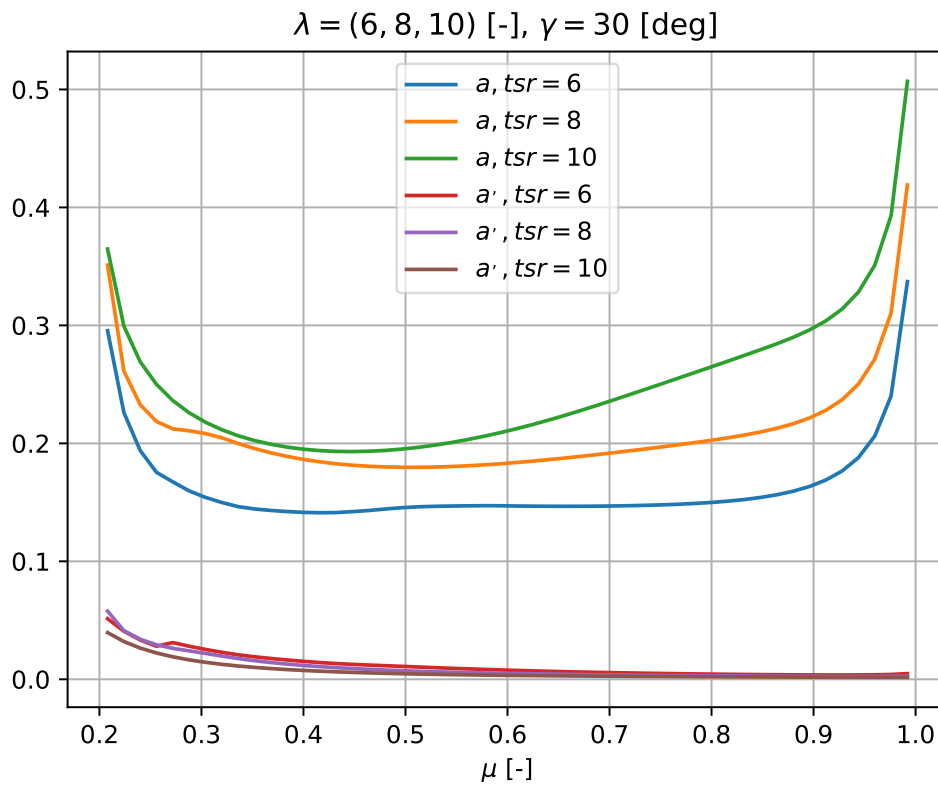


Figure 3.4: Axial and azimuthal inductions at yaw of 30 degrees.

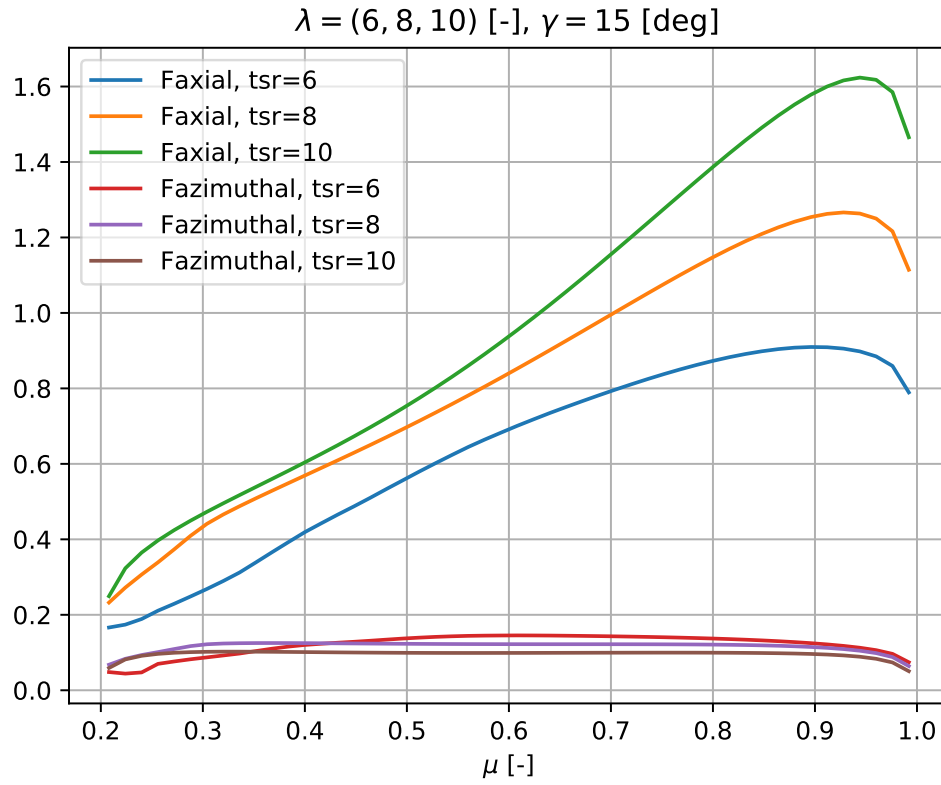


Figure 3.5: Thrust and azimuthal loading normalized by $\frac{1}{2}\rho U_\infty^2 R$.

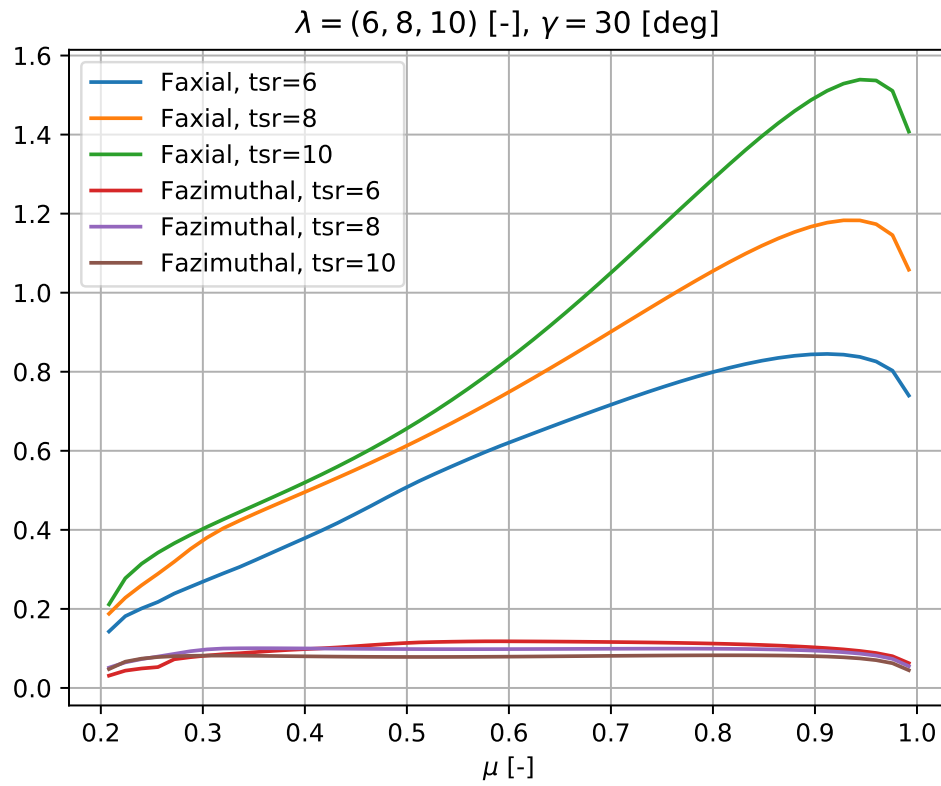


Figure 3.6: Thrust and azimuthal loading normalized by $\frac{1}{2}\rho U_\infty^2 R$.

Table 3.2: CT and CP for yaw angle of 30 degrees.

	tsr 6	tsr 8	tsr 10
CT	0.4404	0.5751	0.6796
CP	0.2837	0.3443	0.3569

The tip correction tries to account for this effect. The expression Prandtl derived for that factor is shown in equation 3.1. Its value over the blade is plotted in Figure 3.11. It relates the induction factor near the blade a_b with the azimuth average a : $a_b = a/f$ [1].

$$f(\mu) = \frac{2}{\pi} \arccos \left[\exp \left(-\frac{B}{2} \left(\frac{1-\mu}{\mu} \right) \sqrt{1 + \frac{\lambda^2 \mu^2}{(1-a)^2}} \right) \right] \quad (3.1)$$

- Power coefficient C_p
 - Tip correction: 0.4528
 - No tip correction: 0.4757
 - Increase: 5.05 %
- Thrust coefficient C_T
 - Tip correction: 0.6581
 - No tip correction: 0.6691
 - Increase: 1.67 %
- Power to thrust ratio C_p/C_T
 - Tip correction: 0.6880
 - No tip correction: 0.7109
 - Increase: 3.32 %

3.4. Influence of numerical discretization **BERNAT**

3.5. Evaluation of stagnation enthalpy **CARLOS**

If heat exchange, viscous forces and compressibility effects are neglected, the flow temperature does not change. Therefore, it can be assumed that the air's internal energy is always constant. Then, the changes in stagnation enthalpy and stagnation pressure are equivalent. The mechanical energy equation (3.2) describes how the stagnation pressure p_t changes. Note that it has been obtained as the scalar product of the momentum equation and the velocity vector.

$$\vec{v} \cdot \vec{\nabla} p_t = \vec{v} \cdot \vec{\nabla} \vec{\tau} + \vec{v} \cdot \vec{b} \quad (3.2)$$

If viscous forces are not considered, $\tau = 0$, the stagnation pressure can only due to the body forces b work. The only domain region where these forces are not null, and therefore, exert some work is the rotor plane. This means that the stagnation pressure only changes across the rotor plane. See equations (3.3) and (3.4) for the stagnation pressure expressions up and down-stream of the rotor plane respectively. They are plotted in Figure 3.12.

$$p_{t_u} = p_a + \frac{1}{2} \rho u_\infty^2 \quad (3.3)$$

$$p_{t_d} = p_a + \frac{1}{2} \rho u_\infty^2 (1 - 2a)^2 \quad (3.4)$$

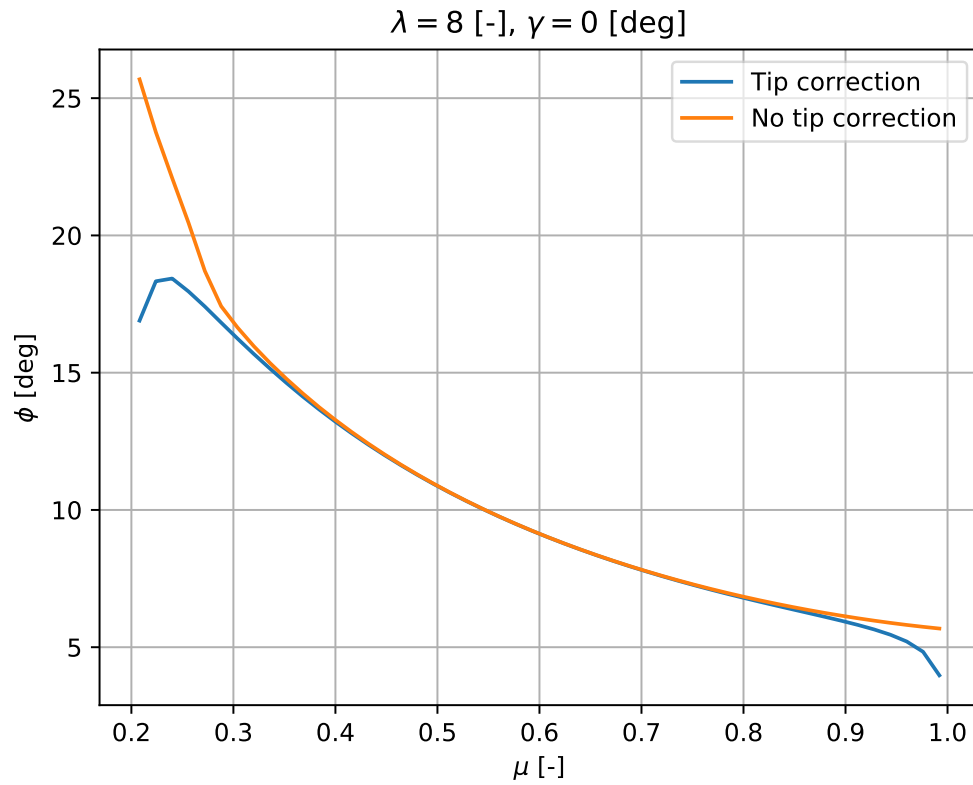


Figure 3.7: Flow angle distribution with and without tip correction.

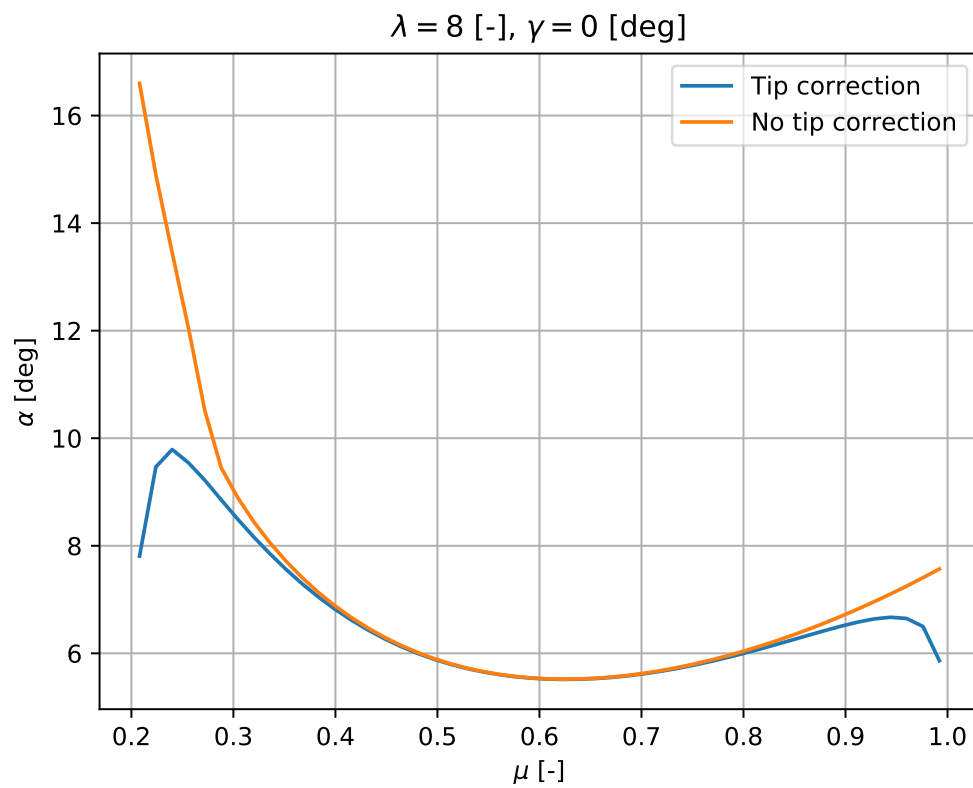


Figure 3.8: Angle of attack distribution with and without tip correction.

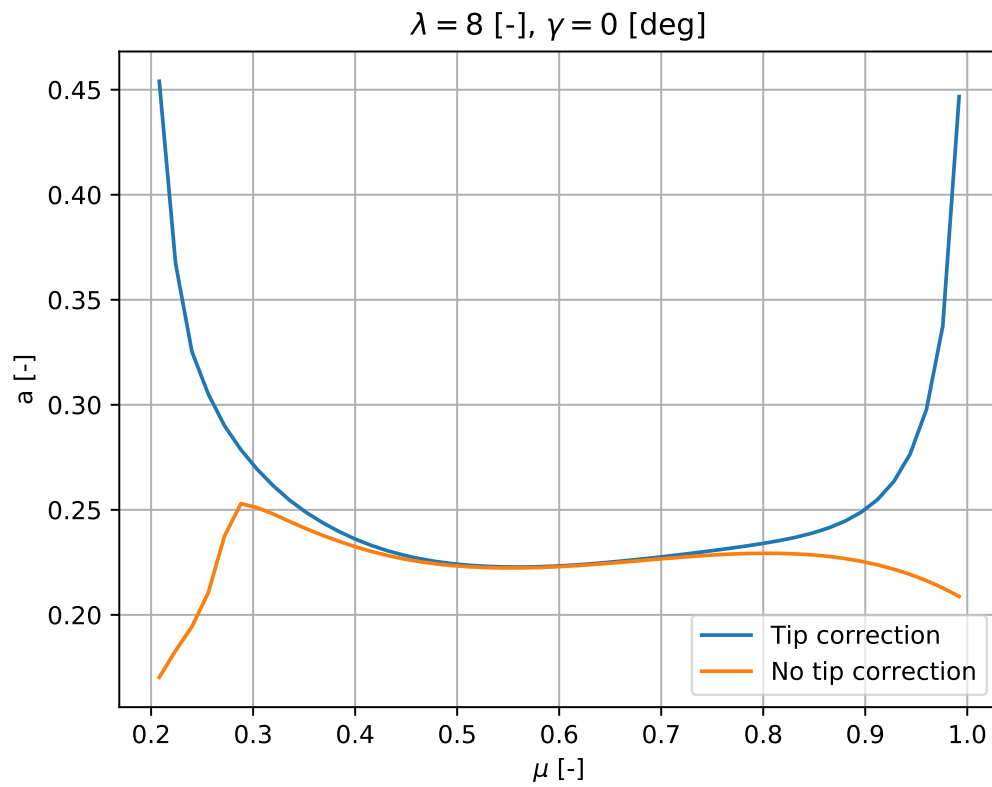


Figure 3.9: Axial induction distribution with and without tip correction.

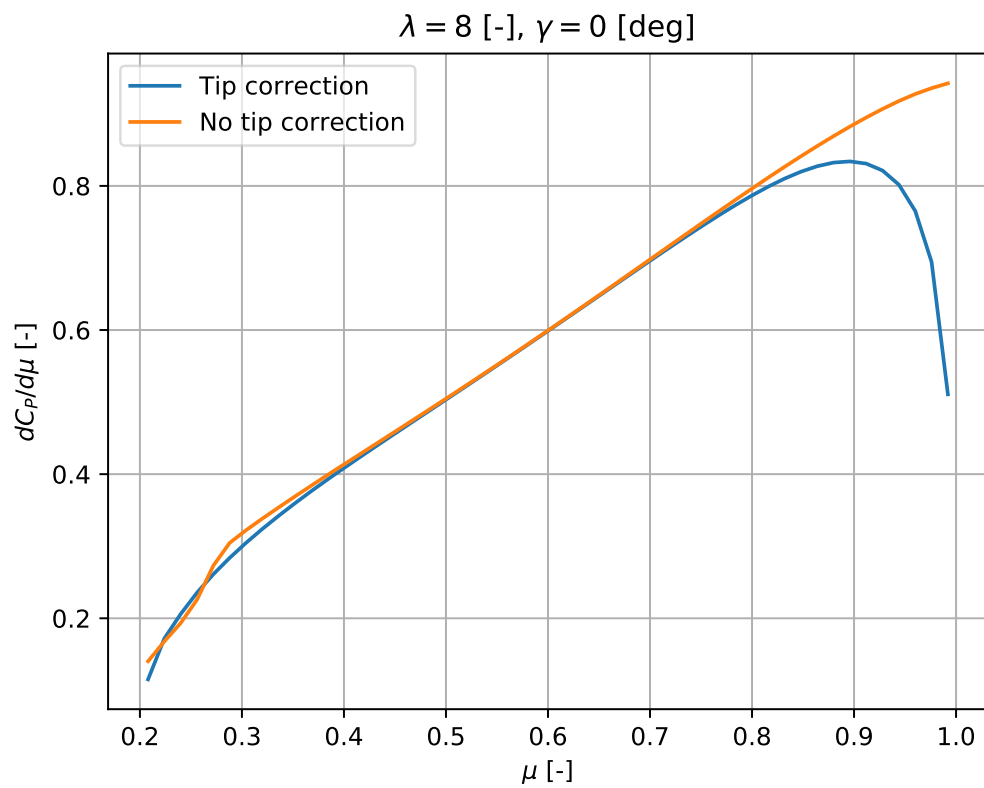


Figure 3.10: Power coefficient distribution with and without tip correction.

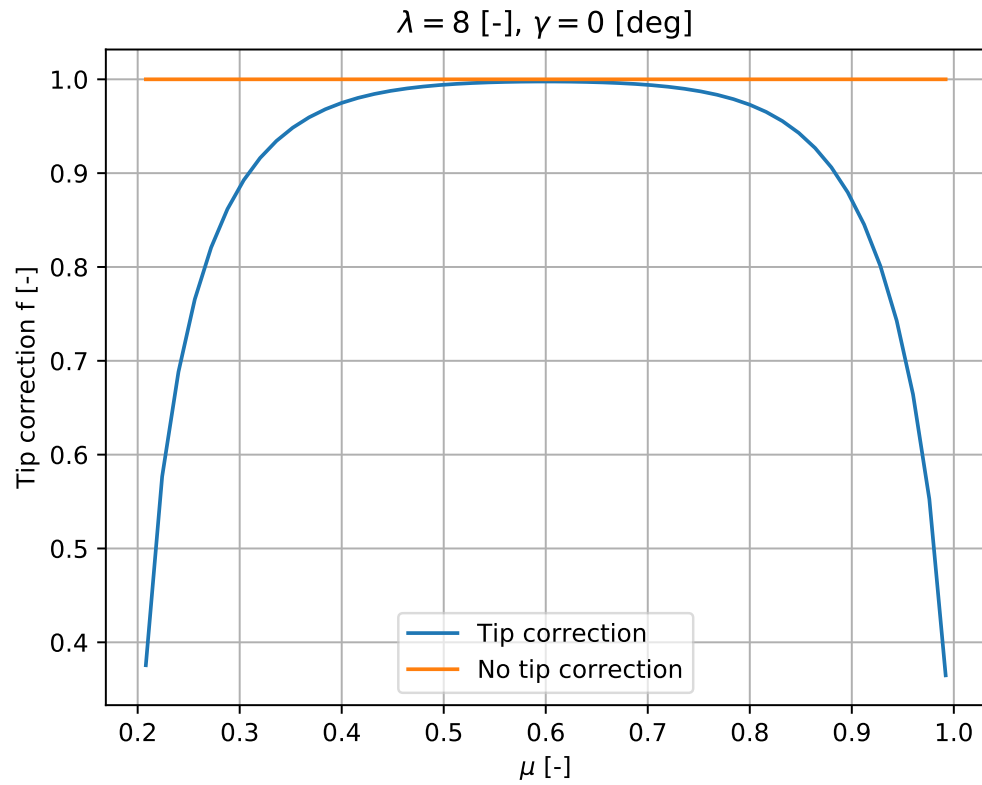


Figure 3.11: Prandtl's tip loss factor distribution with and without tip correction.

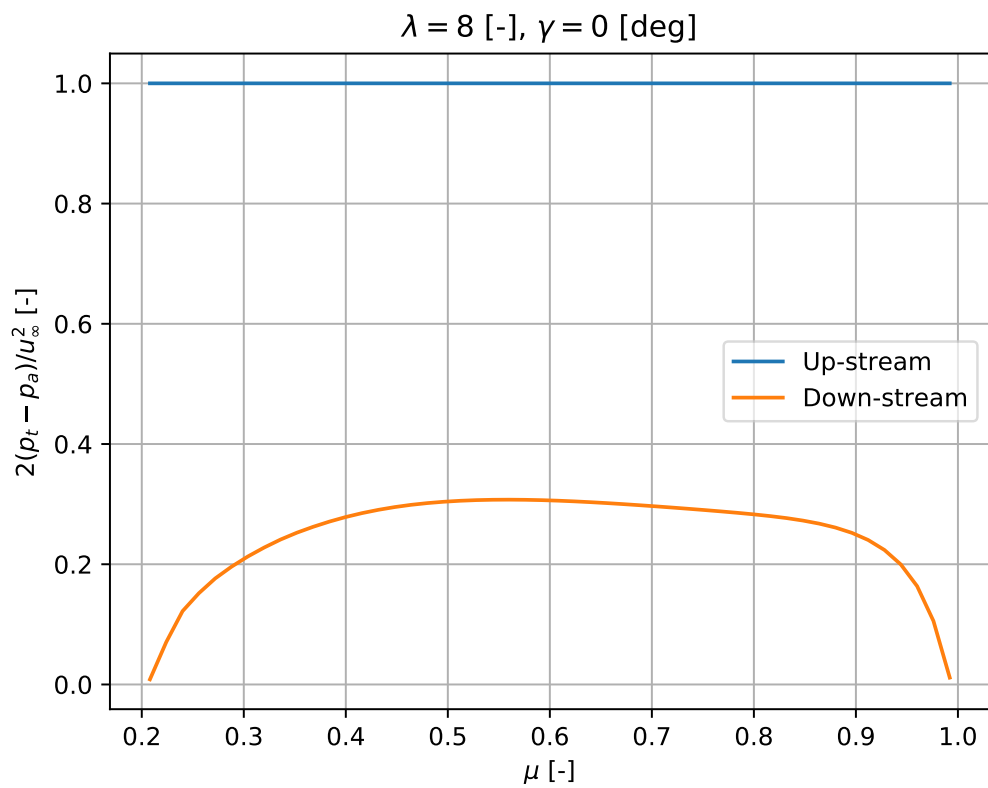
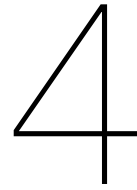


Figure 3.12: Stagnation enthalpy distribution.

3.6. System of circulation and vorticity CARLOS

Plot a representation of the system of circulation. Discuss the generation and release of vorticity in relation to the loading and circulation over the blade.

3.7. Operational point NIKLAS



Optional

4.1. Explanation of the design approach used for maximizing the Cp or efficiency

Blabla

4.2. Plots with explanation of the new designs

Rick Sanchez

5

Conclusions NIKLAS

SHORT discussion/conclusion, including the similarities and differences between the two rotor configurations (yaw vs. aligned rotor), flow field and operation

Bibliography

- [1] Burton, T. and Jenkins, J. and Sharpe, D. and Bossanyi, E. *Aerodynamics of Horizontal Axis Wind Turbines*, chapter 3, pages 39–136. John Wiley & Sons, Ltd, 2011. ISBN 9781119992714. doi: <https://doi.org/10.1002/9781119992714.ch3>. URL <https://onlinelibrary.wiley.com/doi/abs/10.1002/9781119992714.ch3>.